Turk J Phys
36 (2012) , 9 – 21.

doi:10.3906/fiz-1102-1

Structural and optical studies on La doped CdS nanocrystalline films

Kusumanjali DESHMUKH, Mimi MUKHERJEE and Shashi BHUSHAN
Shri Shankaracharya College of Engineering and Technology
Bhilai-490020, C.G., INDIA
e-mail: anjali_d25@rediffmail.com

Received: 01.02.2011

Abstract

This paper reports the synthesis of pure and lanthanum (La) doped nanocrystalline CdS semiconducting films on the glass substrate by means of chemical bath deposition (CBD), with $Cd(CH_3COO)_2$ as Cadmium (Cd) ion source, $(NH_2)_2CS$ as sulphur (S) ion source and Thioglycerol as capping agent. Long, rod like structures is observed in SEM micrographs of the films. XRD studies show the existence of both hexagonal and cubic phases. Increase in FWHM is observed for smaller particle due to nanocrystalline effect. UV-VIS absorption studies show shift of absorption edge towards lower wavelength side. Corresponding change in band gap energy results in shift of photoluminescence edge emission spectra. Also emission peaks near 366 nm are observed under 230 nm excitation due to transitions at higher energy levels.

Key Words: II-VI semiconductors, chemical bath deposition method, photoluminescence spectra, nanocrystalline materials

PACS: 71.55.GS, 61.82.RX, 81.15.L

1. Introduction

Particles with dimensions in the nanometre range, formed of II-VI semiconductors are important nanomaterials for optoelectronic applications. In particular, when the size of nanocrystallites are close to or smaller than the exciton Bohr radius within the corresponding bulk material, they exhibit very special physical and chemical properties [1]. Due to the size dependent quantum confinement, their optical properties like photoluminescence (PL) emission peaks are tunable. The most common II-VI semiconductor nanoparticles, are cadmium chalcogenide nanocrystals (CdTe, CdSe and CdS). Gao et al. [2] found that reactions in presence of thiols (mercaptans), which contain SH group attached to carbon atom, result in surface modification of the nanoparticles and reduction of the non-radiative local surface traps which, in turn, lead to an enhancement of the quantum yield of the excitonic transitions. Thioglycerol is one such thiols and has been found to act as capping agent [3]. Methanol is used as solvent for thioglycerol. II-VI semiconductor nanoparticles have been fabricated by various methods like sol-gel, electrostatic deposition [4, 5], solvent growth [6], DC magnetron sputtering [7] and

chemical deposition [8–11] methods. In the present work La doped CdS photo luminescent nanoparticles have been synthesised by simple Chemical bath deposition (CBD) technique which is a low-cost method, for producing uniform, adherent and reproducible films. It is well known that, depending on the deposition condition, an "ion-by-ion" growth process results in compact and adherent films while a "cluster-by-cluster" process, or colloidal growth, yields porous films [12].

Further, Lanthanide ions possess fascinating optical properties and their discovery, first industrial uses and present high technological applications are largely governed by their interaction with light. Lighting devices (economical luminescent lamps, light emitting diodes), television and computer displays, optical fibres, optical amplifiers, lasers, as well as responsive luminescent stains for biomedical analysis, medical diagnosis, and cell imaging rely heavily on lanthanide ions. Solid materials containing optically active dopants, transition metal or lanthanide ions, find use in a wide variety of technological applications. Applications include lamp, display, and X-ray phosphors, optical-fibre amplifiers, solid-state lasers, and luminescence-based sensors.

A host is usually necessary to dilute the optically active ions and prevent rapid non-radiative processes from occurring, i.e., all of the energy being lost as heat. Hosts are usually insulators, but semiconductors can also serve as hosts for optically active ions, as long as the luminescent excited state does not overlap with the conduction band leading to quenching. Not much work has been reported regarding effect of the first element (La) of Lanthanides. Bhushan et al. [13] reported that PL in La doped (Cd-Pb)S thin films showed emission in green region with peak at 530nm under 365nm excitation. In such bulk films photoconductivity and photovoltaic effects were also reported [14]. To further investigate and establish the role of La in the host nanocrystalline CdS semiconductor, La was selected as impurity for nanocrystalline studies.

The present paper reports results of some nanocrystalline effects observed in pure and La doped CdS films prepared by CBD method using thioglycerol as capping agent. Results of PL spectra under 230nm excitation are reported and discussed along with SEM, XRD and Optical absorption studies.

2. Experimental

2.1. Film preparation

In this study CdS nanocrystalline films were prepared on glass substrate by CBD technique. The microscopic glass slides of dimensions 24 × 75 mm was used as substrates. These slides were first cleaned with H_2SO_4, acetone, double distilled water and ultrasonic cleaner. Then, the dried glass slides were dipped vertically into a mixture of solutions of 1M Cadmium-acetate, TEA, 30% aq. Ammonia and Thiourea. 0.01 M NaF and varied molar concentrations (0.001 M, .005 M, 0.01 M, and 0.05 M) of Lanthanum Nitrate as an impurity were also added to the solution. All solutions were prepared in double distilled water.

Bhushan and co-workers [15, 16] reported that NaF acts as flux as in its absence the inclusion of rare earth impurities were not much effective. Also, it helps in improving crystallinity due to which the emission intensity improves. The capping agent thioglycerol with methanol (TGM) in 1:1 ratio were then added to the original mixture of solutions, since this ratio gave better results. Role of capping agents is to avoid coalescence of particles so as to reduce the particle size. It should be noted that, at room temperature, the precipitation rate was very slow and when the mixture was kept at 60 °C in water bath, precipitation occurred rapidly. The films were then formed on glass substrate by dipping the substrate in this mixture at the temperature of 60 °C in constant temperature water bath for 60 min. The samples were then washed with double distilled water and

dried at room temperature. The pH value of this mixture was found to vary from 11.2 at beginning to 10.9 at the end of deposition.

2.2. Measuring instruments

SEM and XRD studies were made at IUC-DAE, Indore, India, using a JEOL JSM 5600 scanning electron microscope and a Rigaku RUZHR X-Ray diffractometer (CuK_α radiation, $\lambda = 0.154$ nm). The optical absorption spectra were studied by using a Shimadzu (UV-VIS) Pharma Spec-1700 Spectrophotometer. Photoluminescence studies were made by RF 5301, Shimadzu fluoro spectrophotometer.

3. Results and discussion

The films prepared on glass substrate in this study are synthesised by a simple chemical bath deposition approach. The films are deposited as a result of precipitation followed by condensation from a solution of the precursors. Organic molecule "capping agent" Thioglycerol was added in different volumes in order to limit the growth of the particles and control their size [17, 18]. Films deposited on glass substrates were rinsed with double distilled water and dried at room temperature. The samples thus prepared exhibited a change in particle colour from dark yellow in case of thin film (without capping agent) to light yellow, and finally pale yellow for increased volume of TGM in the precursor solution [19]. In films prepared, in the presence of capping agent, shift of PL peaks towards shorter wavelength side has been observed along with improvement in intensity.

To establish the role of La the PL emission, undoped and doped CdS with La were checked under the excitation of 365 nm Hg light. It was observed that undoped CdS shows emission in green yellow region, the intensity of which is found to improve in presence of NaF.The PL emission from CdS:La was comparatively less intense while CdS:NaF,La again showed improvement in intensity with increasing concentration of La. This suggests that more appropriate substitution of La in the lattice. Maximum intensity was found for 0.01 M concentration of Lanthanum Nitrate solution, and thus 0.01 M concentration of Lanthanum Nitrate was selected for the characterization and optical study of nanocrystalline effect. Maximum brightness at particular concentration followed by quenching of emission at higher concentration is indicative of role of impurity, La in the present system.

3.1. SEM studies

The SEM micrographs of undoped and doped CdS films deposited on glass substrate are presented in Figure 1 and Figure 2. Figure 1 shows the morphological features of undoped CdS, CdS:NaF and CdS:NaF,La at 0.2 ml volume of TGM. It is observed that the micrograph of undoped CdS (Figure 1(a)) consists of combination of large number of smaller grains along with rod type structure. In presence of NaF (Figure 1(b)) more dense distribution of grains are seen. Further, due to inclusion of La (Figure 1(c)) morphology changes to platelets/flakes type structure. It has also been observed from absorption studies that the particle size increases (17 nm and 46.6 nm respectively) as compared to undoped CdS films (3.47 nm) in presence of NaF and La, supporting this view. A similar observation has been found from XRD studies as well, i.e. the particle sizes increase in presence of NaF and La.

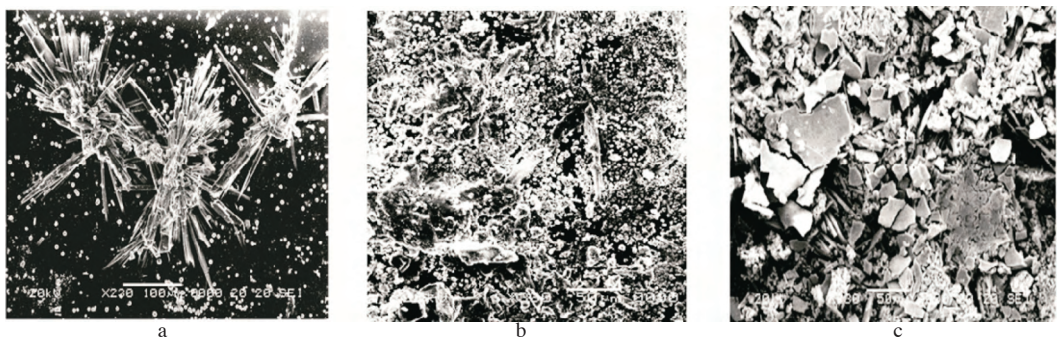

a b c

Figure 1. Effect of La doping on morphological features of different nanocrystalline CdS films with 0.2 ml TGM. Film structure of **(a)** undoped CdS; **(b)** CdS:NaF; and **(c)** CdS:NaF,La.

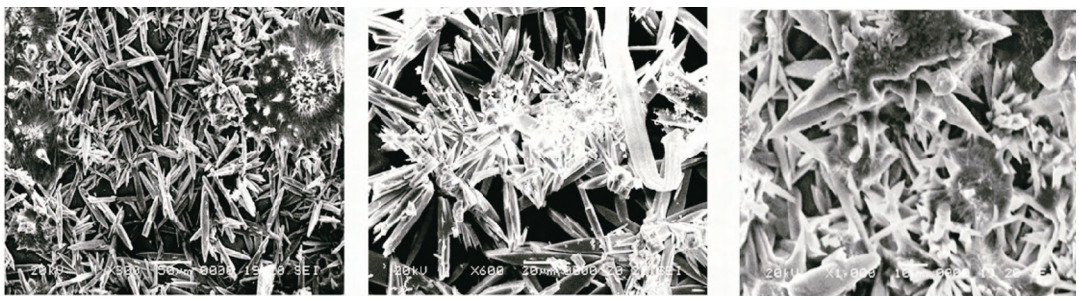

a b c

Figure 2. Effect of La doping on morphological features of different nanocrystalline CdS films with 0.7 ml TGM. Film structure of **(a)** undoped CdS; **(b)** CdS:NaF; and **(c)** CdS:NaF,La.

Figure 2 shows the morphological features of undoped and doped films with 0.7 ml TGM. In Figure 2(a) more developed long nanorods are seen and in Figure 2(b) along with rod type structures, grain type structures are also observed. In Figure 2(c), again, combination of nanorods and platelets type structure is seen. In this case also, absorption studies show that the particle sizes in presence of NaF and La are larger (5.19 nm and 4.43 nm, respectively) than that of undoped film (3.35 nm).

3.2. XRD studies

The X-ray diffractrograms of doped and undoped CdS films are shown in Figure 3. This figure contains results of undoped CdS, CdS:NaF, and CdS: NaF,La in presence of 0.7 ml volumes of TGM. The diffraction lines were assigned by comparing with ASTM data and evaluating lattice constants and comparing with the reported values. It is seen that the diffraction pattern consists of (100), (002), (101), (102), (003), (110), (111) and (103) lines of CdS hexagonal phase. Same peaks with a bit enhanced intensities with no appreciable change in FWHM are observed in the films of CdS:NaF. Although the prime objective of NaF addition to the reaction mixture was the effective incorporation of dopant La in CdS films, it was also observed that the presence of NaF has resulted in better deposition of films under same preparation condition. The films are found to be more uniform and adherent which implies that NaF improves the crystallinity of prepared samples, which might have resulted in enhancement in the intensities of diffraction lines corresponding to $(101)_h$, $(003)_h$, $(110)_h$ planes. Further, doping of La causes disappearance of few lines along with reduction in intensity of all lines except for

$(110)_h$ planes. Thus, it may be inferred that inclusion of La reduces the crystallinity of CdS films. In an earlier work Bhushan and Sharma [20] reported that CdS films show amorphous type behaviour in presence of La.

Figure 4 shows the nanocrystalline effect in the XRD pattern of La doped CdS films for 0.2 ml and 0.7 ml volumes of TGM. Increase in TGM volume in the precursor solution causes broadening of several diffraction peaks. Figure 5 shows broadening of $(210)_c$, $(102)_h$, $(003)_h$ and $(110)_h$ lines. In this figure range of angles is limited from 26° to 46°, so that the broadening can be seen clearly. The corresponding changes in FWHM are presented in Table 1. This is a consequence of particle size reduction.

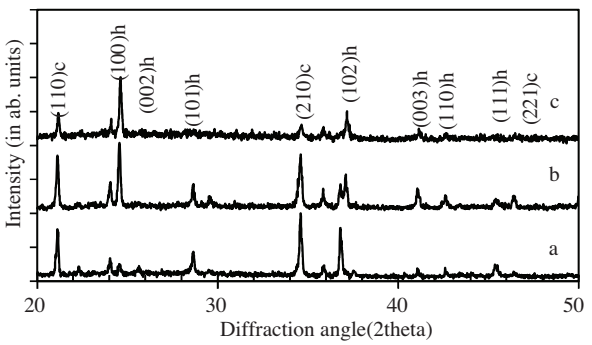

Figure 3. X-ray diffractrograms of various nanocrystalline undoped and doped CdS films; Plot **(a)** is for CdS + 0.7 ml TGM; **(b)** is for CdS:NaF + 0.7 ml TGM; and **(c)** is for CdS:NaF,La + 0.7 ml TGM.

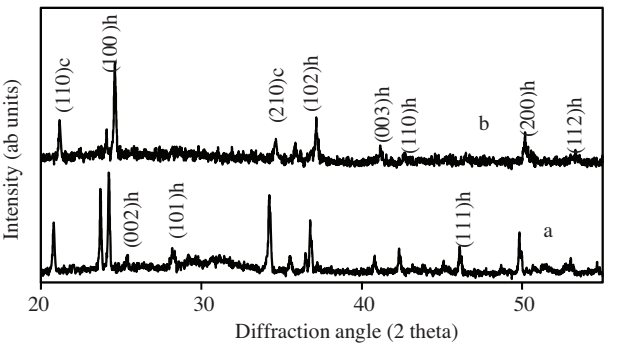

Figure 4. X-ray diffractrograms of some La doped nanocrystalline CdS films. Plot **(a)** is for CdS:NaF,La + 0.2 ml TGM; and **(b)** is for CdS:NaF,La + 0.7 ml TGM.

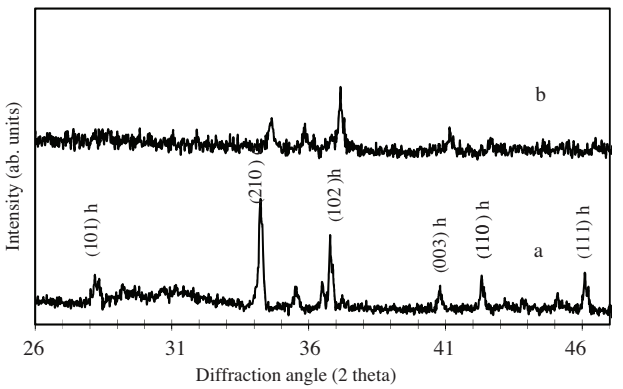

Figure 5. Broadening of diffraction lines (lying within the 2θ range 26°–46°, as seen in Figure (4)) of some La-doped nanocrystalline CdS films. Plot **(a)** is for CdS:NaF,La + 0.2 ml TGM; and plot **(b)** is for CdS:NaF,La + 0.7 ml TGM.

The XRD data of doped and undoped systems along with calculated and standard values of lattice constants are shown in Table 2. As mentioned above, films examined show combination of hexagonal and cubic phases and the values of lattice constants are quite close to reported values. Using the Debye-Scherer's formula [21]

$$L = \frac{0.94\lambda}{\beta_{1/2}\cos\theta} \tag{1}$$

where L is the particle size, λ is the X-ray wavelength used, $\beta_{1/2}$ is the full width at half maxima (FWHM) of

the diffraction peak and θ is the angle of diffraction. Particle sizes were calculated for $(210)_c$, $(102)_h$, $(003)_h$, $(110)_h$ peaks of CdS:NaF,La with 0.2 ml and 0.7 ml volumes of TGM and the corresponding values are as follows: 48 nm, 88 nm, 45 nm, 55 nm and 20 nm, 27 nm, 21 nm, 29 nm at two volumes, respectively. Thus, it is apparent that increasing volume of capping agent enhances reduction in particle size. It should be further noted that according to this formula at constant θ, FWHM ($\beta_{1/2}$) should increase with reduction in particle size as observed in the present case.

Table 1. Full width at half maximum (FWHM) width of diffraction peaks exhibited at two different TGM volumes. Data shows line broadening with increase in TGM.

Diffraction Plane	Full width at half maximum (FWHM) width	
	with 0.2 ml TGM	with 0.7 ml TGM
$(210)_c$	0.18°	0.44°
$(102)_h$	0.10°	0.32°
$(003)_h$	0.20°	0.42°
$(110)_h$	0.16°	0.30°

Table 2. XRD data of different nanocrystalline CdS films (deposition time = 60 min; temperature of deposition = 60 °C).

d value (in Å)		Relative intensities		hkl	lattice const.(in Å)	
Obs.	Reported	Obs.	Reported		Obs.	Reported
CdS + 0.7 ml TGM						
4.2	4.11	77	-	(110)cCdS	a = 5.93	5.818
3.61	3.58	24	75	(100)hCdS	a = 4.17	4.13
3.47	3.35	23	59	(002)hCdS	c = 6.94	6.71
3.31	3.36	18	100	(111)cCdS	a = 5.738	5.818
3.11	3.16	43	100	(101)hCdS	a = 4.17	4.13
					c = 6.14	6.71
2.59	2.58	100	—	(210)cCdS	a = 5.79	5.818
2.44	2.45	78	25	(102)hCdS	a = 4.17	4.13
					c = 6.62	c = 6.71
2.396	2.375	16	—	(211)cCdS	a = 5.73	5.818
2.19	2.23	19	—	(003)hCdS	c = 6.59	6.671
2.12	2.06	20	57	(110)hCdS	a = 4.24	4.13
1.99	1.97	24	—	(111)hCdS	c = 6.677	6.71
1.95	1.93	13		(221)cCdS	a = 5.85	5.818
1.911	1.899	12	42	(103)hCdS	c = 6.75	6.71
CdS : NaF + 0.7 ml TGM						
4.2	4.11	32	—	(110)cCdS	a = 5.93	5.818
3.62	3.58	100	75	(100)hCdS	a = 4.137	4.13
3.11	3.16	41	100	(101)hCdS	c = 6.293	6.71
2.88	2.9	17	40	(200)hCdS	a = 5.78	5.818
2.59	2.6	83		(210)cCdS	a = 5.79	5.818
2.44	2.45	41	25	(102)hCdS	c = 6.673	6.71
2.387	2.375	12	—	(211)cCdS	a = 5.84	5.818

Table 2. Contunied.

d value (in Å)		Relative intensities		hkl	lattice const.(in Å)	
Obs.	Reported	Obs.	Reported		Obs.	Reported
1.99	2.06	20	57	(110)hCdS	a = 4.136	4.13
1.95	1.97	24		(111)hCdS	c = 6.69	6.71
1.77	1.76	17	45	(112)hCdS	c = 6.675	6.71
CdS : NaF, La + 0.2 ml TGM						
3.5	3.58	25	75	(100)hCdS	a = 4.04	4.13
3.165	3.168	31	100	(101)hCdS	c = 6.86	6.71
3.47	3.35	13	59	(002)hCdS	c = 6.9	6.71
2.61	2.6	79	100	(210)cCdS	a = 5.83	5.818
2.44	2.45	57	25	(102)hCdS	c = 6.70	6.71
2.21	2.236	24	—	(003)hCdS	c = 6.63	6.71
2.06	2.068	15	57	(110)hCdS	a = 4.12	4.13
2.006	2.004	20	40	La		
1.968	1.95	32	20	(111)hCdS	c = 6.74	6.71
1.829	1.79	45	17	(200)hCdS	a = 5.783	4.13
1.7265	1.761	22	45	(112)hCdS	c = 6.716	6.71
4.2	4.11	47	100	(110)cCdS	a = 5.9	5.818
CdS : NaF, La + 0.7 ml TGM						
3.61	3.58	100	75	(100)hCdS	a = 4.17	4.13
2.587	2.6	31	—	(210)cCdS	a = 5.78	5.818
2.41	2.45	50	25	(102)hCdS	c = 6.51	6.71
2.19	2.23	24	—	(003)hCdS	c = 6.58	6.71
1.818	1.79	37	17	(200)hCdS	a = 4.18	4.818
2.8	2.79	23	30	La		
3.11	3.16	24	—	(101)hCdS	c = 6.13	6.71

3.3. Optical absorption studies

The optical absorption spectra of different doped and undoped nanocrystalline CdS films deposited on glass substrate by CBD technique show shift in onset of absorption spectra towards the lower wavelength side on addition of TGM (see Figures 6 and 7), which confirms the particle size reduction. For direct band gap materials, the optical absorption coefficient α and the optical bandgap E_g are related by

$$\alpha = c(h\nu - E_g)^{1/2}/h\nu, \tag{2}$$

where c is a constant [22].

Thus, the extrapolation of nonlinear plot between $(\alpha h\nu)^2$ as a function of $(h\nu)$ gives the band gap of the corresponding material. Tauc's $(\alpha h\nu)^2$ vs. $(h\nu)$ plots for La doped nanocrystalline films, are shown in Figure 8, and the values of band gaps evaluated from such plots are summarised in Table 3.

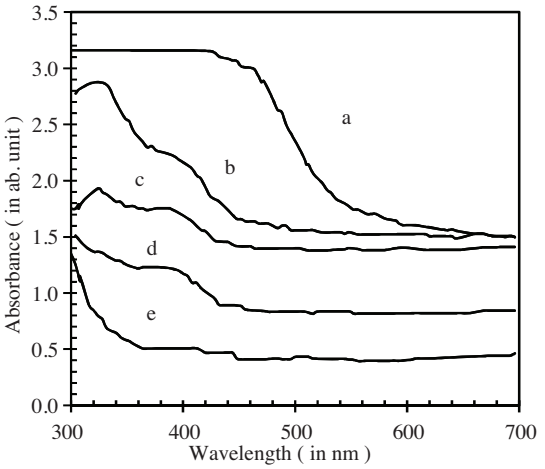

Figure 6. Optical absorption spectra of various undoped CdS nanocrystalline films for (**a**) CdS bulk; (**b**) CdS:NaF + 0.2 ml TGM; (**c**) CdS:NaF + 0.7 ml TGM; (**d**) CdS + 0.2 ml TGM; and (**e**) CdS + 0.7 ml TGM.

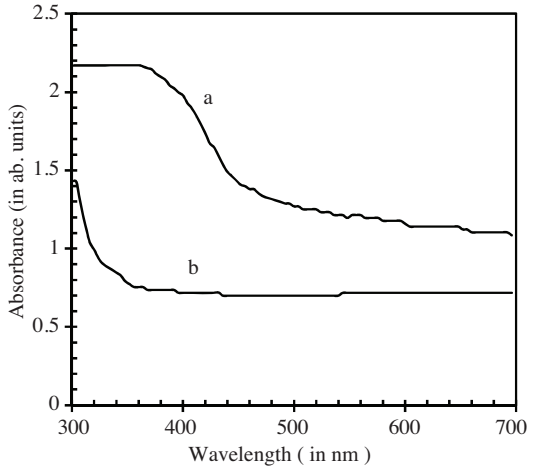

Figure 7. Optical absorption spectra of different La doped CdS nanocrystalline films for **(a)** CdS:NaF,La + 0.2 ml TGM; (**b**) CdS: NaF,La + 0.7 ml TGM.

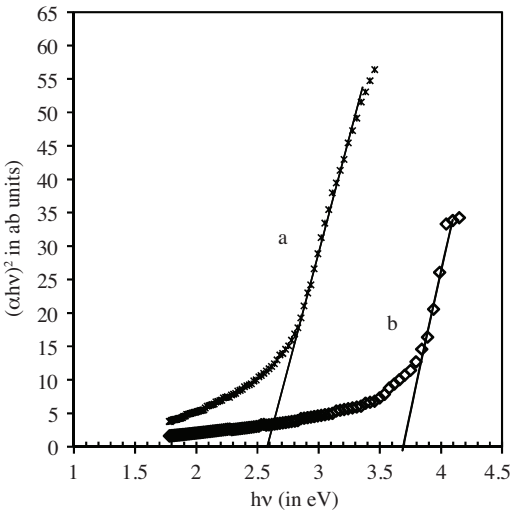

Figure 8. Tauc's plots of $(\alpha h\nu)^2$ as a function of $(h\nu)$ for La doped CdS nanocrystalline films derived from solutions **(a)** CdS:NaF,La + 0.2 ml TGM; and (**b**) CdS:NaF,La + 0.7 ml TGM.

It is observed that the band gap of undoped CdS films increases from 2.32 eV (bulk) to 3.79 eV (with 0.2 ml TGM) and 3.85 eV (with 0.7 ml TGM). In presence of NaF the increase in band gap was less i.e. 2.43 eV (with 0.2 ml TGM) and 3.48 eV (with 0.7 ml TGM) as compared to undoped CdS. This is probably due to the reason that 0.2 ml and 0.7 ml TGM volume was added in the comparatively increased volume of the reaction mixture. The volume of reaction mixture increases due to addition of appropriate volume of aq. solution of NaF. It should be noted that the volume of original mixture (41 ml) increases from 41.2 ml to 41.7 ml due to addition of two volumes of TGM. Thus, the TGM concentration increases from 0.485% to 1.67%. Due to addition of NaF (12 ml) in the original mixture the TGM concentration increases from 0.376% to 1.30%. The

change in band gap is dependent on the particle size, i.e. increase in band gap due to reduction in particle size which is dependent on the concentration of TGM. Therefore, the observed results are quite in accordance with the increased volumes. Similar effect occurs with inclusion of La also, proportionate change in band gap is comparatively less, i.e. 2.34 eV (with 0.2 ml TGM) and 3.48 eV (with 0.7 ml TGM) because of the increase in total volume of the reaction mixture due to further addition of aq. solution of Lanthanum Nitrate.

Table 3. Calculated values of band gap and particle sizes of various nanocrystalline CdS films.

Systems	Band gap (in eV)	Particle size (in nm)
CdS (bulk)	2.32	—
CdS + 0.2 ml TGM	3.79	3.47
CdS + 0.7 ml TGM	3.85	3.35
CdS:NaF +0.2 ml TGM	2.62	17
CdS:NaF + 0.7 ml TGM	3.31	5.19
CdS:NaF,La + 0.2 ml TGM	2.43	46.7
CdS:NaF,La +0.7 ml TGM	3.48	4.43

It is apparent from all these observation that the band gap of material increases with increasing volume of TGM. Since the coalescence of particles is avoided, the particle size is expected to reduce more and more at higher volume of capping agents. Particularly, for thiophenol this kind of effect was reported by Herron and co-workers [23]. Such kind of absorption also supports the quantum confinement effect in nanocrystalline materials in which the electrons, holes and excitons have limited space to move and their motion is possible for definite values of energies. An important consequence of quantum confinement is blue shift in absorption spectrum (and hence in PL emission spectrum) which results due to increase in band gap of the materials. The particle size can be calculated from bandgap of material using effective mass approximation, given by the formula

$$E_{\mathrm{gn}} = E_{\mathrm{gb}} + \frac{h^2\pi^2}{2\mu R^2}, \tag{3}$$

where E_{gn} is the band gap of nanocrystallites, E_{gb} is the band gap of the bulk semiconductor, R is the radius of particles and μ is the effective mass of electron [24] ($\mu = 0.08\,m_e$, in present case where m_e is the rest mass of electron [25]) in the CdS crystal. The calculated values of particle size for CdS films at varied TGM volumes are also quoted in the Table 3. As expected, the band gap of material increases with increasing volume of TGM since the particle size is reduced and is found to be well in the nano region.

3.4. Photoluminescence studies

The room temperature PL emission spectra of doped and undoped CdS nanocrystalline films at lower volume (0.2 ml) of TGM for the excitation wavelength of 230 nm are shown in the Figure 9. The spectra generated due to such high energy photons display strong peaks centred at around 366 nm and 462 nm. This suggests a shift in emission peak to the shorter wavelength side in the case of nanocrystalline films of CdS in comparison to that of CdS (512 nm; 2.42 eV) for thin films. The strong and narrow emission peak at 462 nm may be due to the band to band transition, which occurs due to blue shift of emission of undoped CdS and thus should correspond to the increased band gap of CdS. This undoubtedly confirms the quantum confinement in the prepared samples. Under nanocrystalline effect two prominent observations are made (a) change in band

gap i.e. its increase with reducing particle size (b) discreteness in the continuum of valence and conduction bands. Maleki et al. [26, 27] have reported that apart from the band emission, discreteness of energy states result in the transitions at higher levels which may cause emission in the shorter wavelength side. The peak near 366 nm may be attributed to a higher level excitonic emission caused due to quantum confinement. The excitonic energy is calculated to be 3.38eV. Devi et al. [28] reported a peak in nanocrystalline CdS at 376 nm with similar explanation. Maleki et al. observed a peak at 340 nm in CdS nanoparticles through 220 nm excitation wavelength, which was related to higher level transitions in CdS crystallites. According to them this kind of band edge luminescence is caused by recombination of excitons and /or shallowly trapped electron- hole pairs. It may be noted that PL edge emission in CdS was extensively investigated by number of workers [29–31] and was associated with excitonic transitions or defect exciton complexes [32].

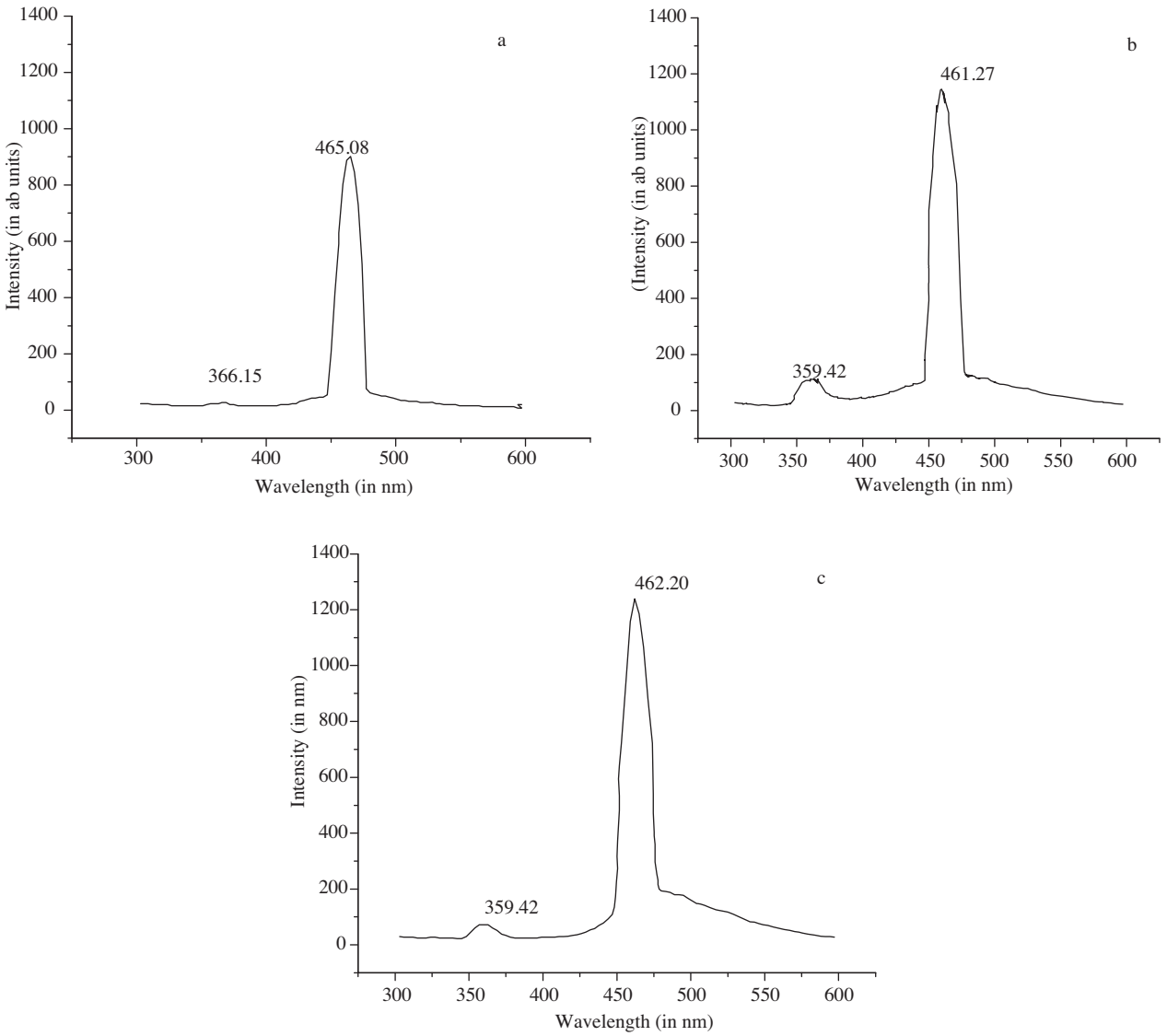

Figure 9. Effect of La doping on PL emission spectra, under 230 nm excitation, for different CdS nanocrystalline films at 0.2 ml TGM volume**: (a)** undoped CdS; **(b)** CdS:NaF; and **(c)** CdS:NaF,La.

As observed from Figure 9(b), addition of NaF in the mixture of solutions improves the intensity of the emission peaks which might be due to the improvement in crystallinity as is also noticed from XRD patterns. Further, increase in emission intensities due to La doping (see Figure 9(c)) may be due to transfer of energy from transitions in its energy levels.

Figure 10 shows effect of doping on PL emission spectra of different CdS nanocrystalline films with increased TGM volume under 230 nm excitation. It can be observed from the figure that due to increase in TGM volume, in the reaction mixture, the films show enhanced PL emission peak at around 360 nm along with broadening of the other peak at 462 nm. Appearance of multiple emission peaks in the shorter wavelength side in undoped CdS films (Figure 10(a)) at 324 nm, 353 nm and 362 nm may be due to transitions at higher energy levels involving excitons. In presence of La, however, the doublet structure at shorter wavelengths disappears (Figure 10(b) and 10(c)) due to compensation of defects in their presence. Improvement in intensity in presence of La may be again associated with transfer of energy from transitions in energy levels of La.

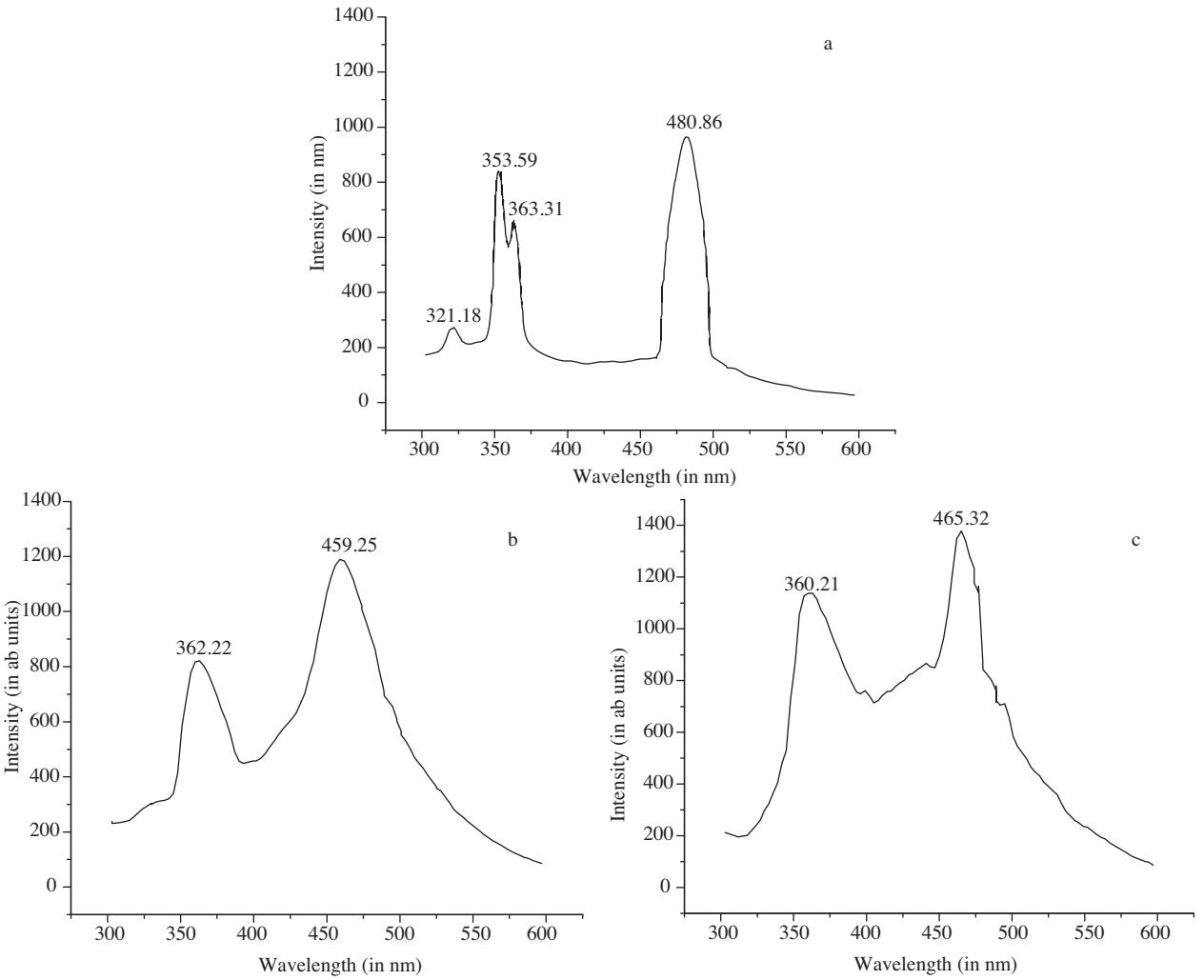

Figure 10. Effect of La doping on PL emission Spectra of different CdS nanocrystalline films at 0.7 ml TGM volume under 230 nm excitation: **(a)** undoped CdS; **(b)** CdS:NaF; and **(c)** CdS:NaF,La.

4. Conclusions

Efficient luminescent material with emission in near UV and visible blue regions under 230 nm excitation can be prepared by simple and low cost technique of chemical bath deposition. As the volume of TGM in the reaction mixture play a vital role in the preparation of doped and undoped nanocrystalline CdS films by this technique, efficient photo luminescent La doped nanocrystalline CdS films have been prepared by optimising the concentration of Lanthanum Nitrate in the precursor solutions. SEM studies on pure and La doped nanocrystalline CdS films show cluster of long, rod like structures at higher volume (0.7 ml) of TGM. XRD studies show existence of both hexagonal and cubic phases in all the systems. Presence of NaF in the reaction mixture causes improvement in crystallinity of films, while reduction in crystallinity is observed with the inclusion of La in CdS. At higher volume of TGM increase in FWHM of XRD peaks is observed suggesting a further reduction in particle sizes. The shift in onset of absorption spectra towards lower wavelength side in presence of TGM supports quantum confinement effect. Shift in PL emission spectra along with appearance of new peaks at shorter wavelength side arise due to this confinement effect. Enhancement in PL emission spectral peaks is observed which may be due to better crystallinity in presence of NaF. Further improvement in PL intensity in presence of La in appropriate concentration appears due to transfer of energy from transitions in La.

Acknowledgements

The authors are grateful to Mr. Ram Janay Choudhary and Mr. V. K.Ahirey IUC-DAE Indore, India, for XRD and SEM studies. We are also thankful to Dr. Nathani and Mr. Avinash Soni, Seed Biology Lab, Pt. R. S. Univ., Raipur India for making PL Studies. One of the authors M. Mukherjee is thankful to DST, New Delhi, India for the financial support through DST-FIST project.

References

[1] L. E. Brus, *J. Chem. Phys.,* **80**, (1984), 4403.

[2] M. Gao, S. Kirstein, H. Möhwald, A. L. Rogach, A. Kornowski and A. Eychmüller, H. Weller, *J. Phys. Chem.*, **102**, (1998), 360.

[3] J. Nanda, A. Kuruvilla, K. V. P. M. Shafi and D. D. Sharma, *Physics of Semiconductor Nanostructures*, ed. K. P. Jain, (Narosa Pub.House, India. 1997).

[4] O. V. Salata, P. J. Dobson, P. J. Huu and J. L. Hutchishon, *Thin solid films*, **251**, (1994), 1.

[5] L. Bakueva, S. Mustukhin, M. A. Hiens, T. W. F. Chan, M. Tzolov, G. D. Scholes and E. H. Sargent, *Appl. Phys. Lett.*, **82**, (2003), 2895.

[6] L. Spanhal, N. House, H. Weller and J. Henglein, *J. Am. Chem. Soc.*, **109**, (1987), 649.

[7] R. Pal, D. Bhattacharya, A. B. Maity, S. Chaudhary, and A. K. Pal, *Nanostruct. Mat.*, **4**, (1994), 329.

[8] S. Mann, A. J. Sharnulis and R. J. P. Willians, *Isr. J. Chem.,* **21**, (1982), 3.

[9] L. Pintia, E. Pential, I. Pintilie, and T. Bobila, *Appl. Phys. Lett.*, **76**, (2000), 1890.

[10] S. Bhushan and S. K. Sharma, *J. Phys. D-Appl. Phys.*, **23**, (1990), 909.

[11] S. Bhushan, M. Mukherjee, and P. Bose, *Rad. effects and defects in solids*, **153**, (2002), 367.

[12] Zhu Yuming, Mao Duli, D. L. Williamson and J. U. Trefny, *Mat. Res. Symp. Proc.*, **426**, (1996), 227.

[13] S. Bhushan, M. Mukherjee and P. Bose, *J. Mat. Sc.(Mat. In Electronics)*, **13**, (2002), 581.

[14] T. Chandra and S. Bhushan, *J. Mat. Sc.*, **39**, (2004), 6303.

[15] S. Bhushan and S. K. Sharma, *J. Mat. Sci. [Mat. in Electronics],* **1**, (1990), 165.

[16] S. Bhushan and S. K. Sharma, *J. Phys. Condens. Matter*, **2**, (1990), 1827.

[17] U. Winkler, D. Eich, Z. H. Chen, R. Fink, S. K. Kulkarni and E. Umbach, *Chem. Phys. Lett.,* **206**, (1996), 95.

[18] M. Kundu, A. Khosravi, P. Singh and S. K. Kulkarni, *J. Mater. Sci.,* **32**, (1997), 245.

[19] Kumpf Christin, *Appl. Phys. A.,* **85**, (2006), 337.

[20] S. Bhushan and S. K. Sharma *Crystal Res.Technol.*, **27**, (1992), 555.

[21] Liu Jinsong, Jieming Cao, Ziquan Li, Guangbin Ji, Shaogao Deng, and Mingbo Zheng, *J. Mat. Sci.*, **42**, (2007), 1054.

[22] A. L. Dawer, P. K. Shishodia, J. Chouhan, G. Kumar, and A. Mathur, *Mat. Sci. Lett.*, **9**, (1990), 547.

[23] N. Heron, Y. Wang and H. Eckert, *J. Am. Chem. Soc.*, **112**, (1990) 1322.

[24] N. Caponitte, L. Peddone, D. Chillura Martino, V. Panto, and V. T. Liveri, *Material Sci Engineer. C.*, **23**, (2003), 531.

[25] Liu Jinsong, Cao Jieming, Li Ziquan, Ji Guangbin, Deng Shaogao and Mingbo Zheng, *J. Mat. Sci.*, **42**, (2007), 1054.

[26] M. Maleki, M. Ghamsari, M. Sasani, S.H. Mirdamadi and R. Ghasemzadeh, *Semicond. Phys. Quant. Elect. & Opto Ele.,* **10**, (2007), 30.

[27] W. Wang, Y. Geng, P. Yan, F. Liu, Y. Xie and Y. Qian, *Inorg. Chem.Communs.,* **4**, (2001), 208.

[28] R. Devi, P. K. Kalita, P. Purkayastha and B. K. Sharma, *Indian J.Phy.*, **82**, (2008), 707.

[29] R. E. Halsted, and M. Aven, *Phys. Rev. Lett.,* **14**, (1965), 64.

[30] S. Iida, and M. Toyoma, *J. Phys. Soc. Jpn.,* **31**, (1971), 190.

[31] Y. Kokobun and T. Kaeriyama, *J. Appl. Phys. Jpn.*, **14**, (1975), 1403.

[32] D. G. Thomas and J. Hopfield, *J. Phys. Rev.*, **128**, (1962), 2135.